Letter to the Editor

Multinodular intraventricular lymphoplasmacyte-rich meningioma with significant calcification: a case description

Guo Li[1], Fa Wu[1], Ju Huang[1], Feizhou Du[1], Junfeng Zhang[1], Zhiwei Zuo[1], Rui Jiang[1], Hailong Yun[2], Peng Wang[1]^

[1]Department of Radiology, The General Hospital of Western Theater Command, Chengdu, China; [2]Department of Pathology, The General Hospital of Western Theater Command, Chengdu, China

Correspondence to: Peng Wang, MD. Department of Radiology, The General Hospital of Western Theater Command, No. 270, Tianhui Road, Rongdu Avenue, Jinniu District, Chengdu 610083, China. Email: kl415@qq.com.

Submitted Nov 22, 2022. Accepted for publication Jun 05, 2023. Published online Jun 15, 2023.
doi: 10.21037/qims-22-1299
View this article at: https://dx.doi.org/10.21037/qims-22-1299

Introduction

Lymphoplasmacytic-rich meningiomas (LPRMs) are clinically rare, are classified as grade I by the World Health Organization (WHO) (1), account for 0.51% of intracranial meningiomas (2), and are characterized pathologically by a large infiltration of lymphocytes and plasma cells within the underlying fibrous structures (3). Here, we present a case report of multinodular LPRM originating from the lateral ventricles, which has not been previously reported in the literature.

Case presentation

All procedures performed in this case report were in accordance with the ethical standards of the institutional and/or national research committee(s) and with the Helsinki Declaration (as revised in 2013). Written informed consent was obtained from the patient for publication of this case report and accompanying images. A copy of the written consent is available for review by the editorial office of this journal.

A 65-year-old Chinese woman presented to the outpatient clinic complaining of persistent unsteadiness in walking and memory loss for more than 4 months with no limb weakness or vomiting. She had been treated for cervical spondylosis at another hospital for 3 months with no improvement. The patient denied any family history of reproductive disease.

On physical examination, the patient was clear-headed, fluent in speech, and able to answer basic questions. The Glasgow Coma Scale (GCS) score was 15. Bilateral pupils were equal in size (3 mm), sensitive to light reflex, and had normal eyelid closure. There was no deflection of tongue extension. Bilateral limb muscle strength was grade V, and muscle tone was normal. The superficial sensation was normal, and no pathological reflexes were evoked.

Computed tomography (CT) showed multiple round high-density nodules in the right ventricle, some with significant calcification and hydrocephalus (*Figure 1A*).

Magnetic resonance imaging (MRI) showed multiple nodular masses with rough edges in the parietal wall of the temporal side, thalamus, and right occipital horn, with obvious peripheral cerebral edema; T1-weighted imaging (T1WI)/T2WI of these nodules included mainly intermediate, but uneven signals, and temporal horn of the right ventricle was enlarged with the surrounding brain parenchyma being edematous (*Figure 1B*,*1C*). Most lesions appeared obvious and unevenly strengthened after enhancement, and the nodules near the right ventricle occipital angle were less fortified (*Figure 1D-1F*).

^ ORCID: 0000-0002-2080-5215.

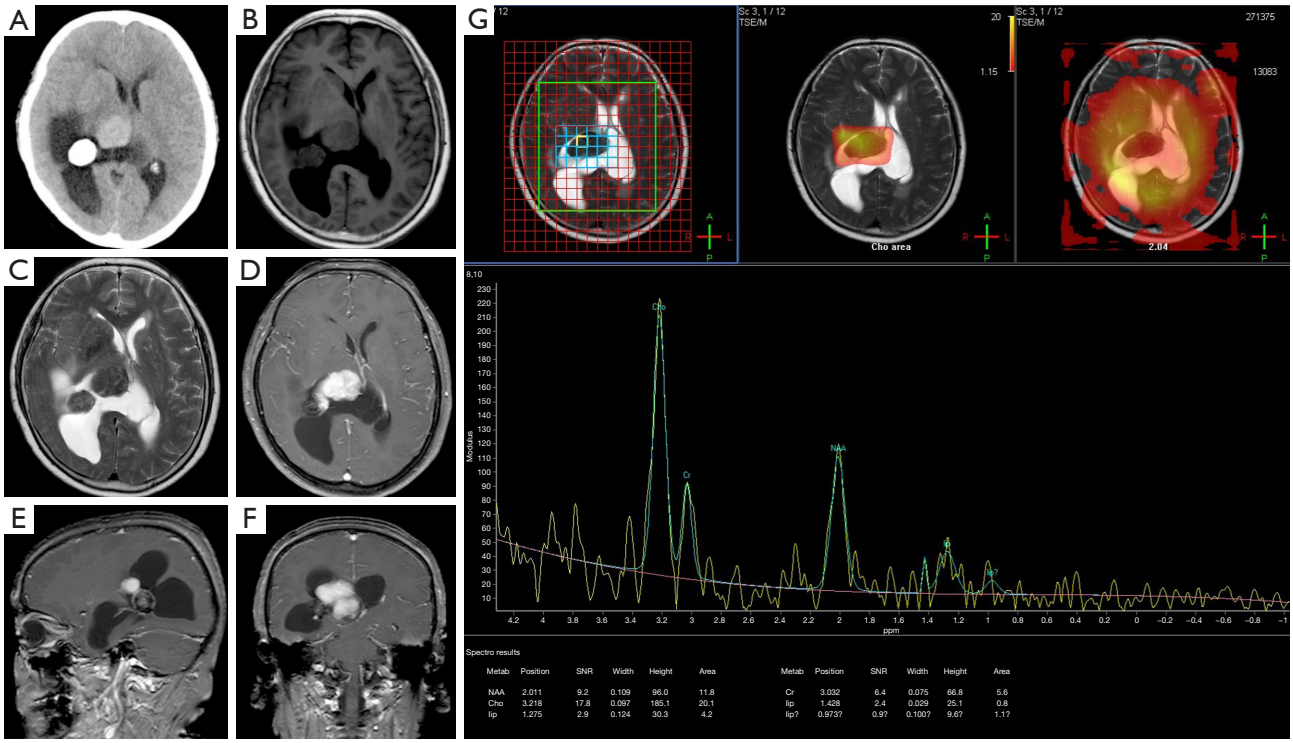

Figure 1 Neuroimages of multinodular intraventricular LPRM. (A) CT revealed multiple slightly hyperdense nodules in the right lateral ventricle, some nodular calcifications, and enlarged hydrocephalus of the ventricular system. (B,C) T1WI and T2WI showed multiple nodules on the temporal side, thalamus, and parietal wall of the right occipital angle, and the signal intensity of these nodules was uneven; the T1WI/T2WI medium signal was dominant, with rough edges and obvious peritumoral edema. (D-F) CE T1WI showed obvious and uneven strengthening of the thalamic side nodules at multiple angles, and less strengthening in the components of the occipital angle side nodules. (G) MRS revealed that the N-acetyl aspartate peak of a large nodule near the right thalamus decreased, and the choline and creatinine peaks increased. LPRM, lymphoplasmacyte-rich meningioma; CT, computed tomography; T1WI, T1-weighted imaging; T2WI, T2-weighted imaging; CE, contrast-enhanced; MRS, magnetic resonance spectroscopy; SNR, signal-to-noise ratio; NAA, N-acetylaspartate.

Under magnetic resonance (MR) spectroscopy, N-acetyl aspartate peaks near the right thalamic nodules decreased and choline and creatinine peaks increased (*Figure 1G*). Based on imaging, we diagnosed this as ependymoma in the lateral ventricle.

After obtaining the patient's consent and completing the relevant preoperative examination and evaluation, the patient underwent a craniotomy, and gross total resection was attained. The surgical procedure mainly includes intracerebroventricular tumor resection, craniotomy intracranial decompression, and cerebrospinal fluid leak repair.

The surgical records for intraoperative findings are described below. We chose the craniotomy route to the right temporal occipital triangle on this patient. The scalp, subcutaneous tissue, temporalis muscle, and periosteum were separated sequentially to fully expose the skull. The power system was introduced, the skull was fixed by turning the hole, and then the skull was milled into an arc with a milling knife. Following this, the bone flap was removed to form a bone window of about 8 cm × 8 cm in size. A cross-shaped "+" incision was made on the dura mater. The cortex of the middle occipital gyrus of the right occipital lobe was incised with the assistance of a microscope and gradually peeled off about 2 cm deep to facilitate entry into the occipital horn of the right lateral ventricle under neuron navigation positioning. The tumor was grayish-white in color and had a relatively hard texture with an intact capsule; the tumor body was well demarcated from the temporal horn and parietal wall of the right lateral ventricle and closely adherent to the lateral wall of the lateral ventricle and the lateral wall of the mesial thalamus. We

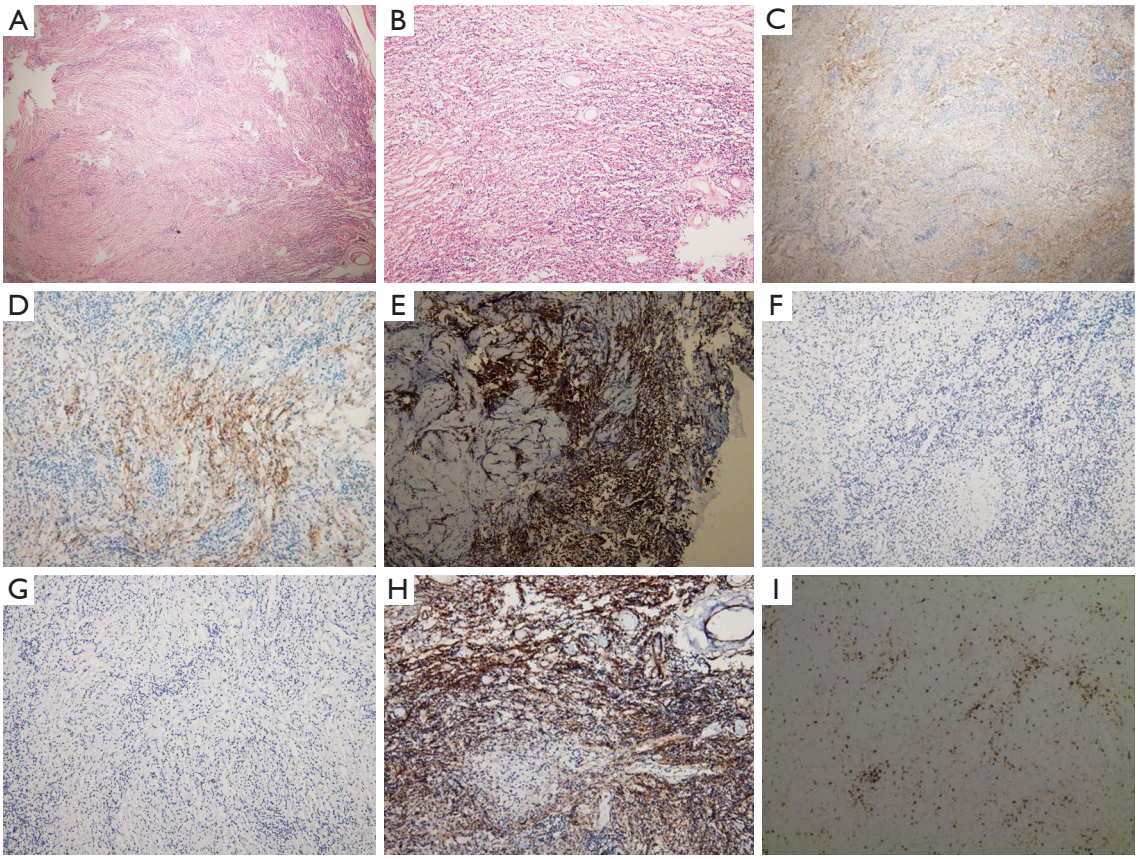

Figure 2 Histopathological changes of the lesion. (A,B) HE staining (A, 40×; B, 100×): the mass lesion showed scattered meningothelial cells and spindle cells arranged in fascicles and vortexes with a surrounding infiltrate of numerous lymphocytes and plasma cells on an overall background of inflammatory cell infiltration. (C-I) Immunohistochemical staining of tumor cells showed that EMA (C, 40×; D, 100×) was positive, LCA-CD45 (E, 40×) was positive, and a large number of lymphocytes could be seen in the background of the picture (stained part). PR (F, 100×) was negative, GFAP (G, 100×) was negative, Ki-67 (H, 10×) was positive (<1%), and vimentin (I, 100×) was positive. HE, hematoxylin and eosin; EMA, epithelial membrane antigen; LCA, leukocyte common antigen; PR, progesterone receptor; GFAP, glial fibrillary acidic protein.

used electrocoagulation to stop the bleeding in the operative area, covered the wound with hemostatic cotton after using saline rinses, and then carefully sutured the dura mater. The dura mater was closed mainly by suturing, and the portion of the defect that formed the cerebrospinal fluid leak was repaired with artificial meninges. Finally, drains were placed in the lateral ventricle and epidural space, respectively. The bone flap was reapproximated with 3 cranial locks, and the galea aponeurotica and skin were sutured in layers. A dressing was applied at the end of the surgery.

During piecemeal resection of this tumor, we found that it had an extremely rich blood supply and crude veins and had wrapped around the right intracerebral veins. Finally, after multiple segmented resections and careful boundary separation, the tumor was completely removed, with intraoperative bleeding of about 300 mL.

Concerning pathological findings, the right ventricle showed WHO grade I LRPM, and the tumor cells showed the following: epithelial membrane antigen (+), glial fibrillary acidic protein (GFAP; –), progesterone receptor (PR; –), leukocyte common antigen (LCA)-CD45 (+), vimentin (+), cytokeratin 5/6 (–), smooth muscle actin (–), S-100 (–), Langerhans (–), and Ki-67 (+, <1%) (*Figure 2*).

Follow-up

The patient recovered well after the operation, rose out of bed independently on postoperative day (POD) 7,

and was discharged on POD 15. Two months later, her preoperative symptoms had completely disappeared, and no residual tumor or recurrence was found on MRI at 24 months' follow-up; she was very satisfied with the treatment outcome.

Discussion

LPRM originates primarily from arachnoid granulosa cells in the brain, is a WHO grade I condition, and is one of the rarest subtypes of meningiomas, characterized by tumor and diffuse lymphocyte and plasma cell infiltration and fibrous tissue hyperplasia in the interstitium (4,5). LPRM is more common in young adults (average age of onset 45 years), and the ratio of male to female incidence is about 1:1.7 (3). The onset sites include the convexity of the brain, the falx cerebri, the cerebellopontine angle, the foramen magnum, the anterior skull base, and the jugular foramen area, among others (5). The common clinical symptoms are intracranial hypertension (headache, dizziness, vomiting, etc.), which can be accompanied by hematopoietic system diseases (anemia, polyclonal-immunoglobulinopathy, etc.) (6).

There are few reports of intraventricular LPRM, which originates mainly from the interstitial or choroidal tissue of the choroid plexus and often occurs in the atrium where the choroid plexus is rich (7). This patient represents a rare case of intraventricular multinodular LPRM, for which the clinical symptoms were mainly memory loss, and the signs of intracranial hypertension were not obvious. Intraventricular meningioma caused the entrapment of the temporal horn of the right lateral ventricle leading indirectly to localized hydrocephalus and periventricular edema, which could have caused memory loss in turn. We speculate that the tumor mainly grows in the right ventricle, and the growth space in this area is relatively large, so there will be no cerebrospinal fluid circulation disorders in the early stage, so the course of the disease is generally longer, and the symptoms of related intracranial hypertension will not appear prematurely. However, if the tumor appears in the third or fourth ventricles, symptoms of increased intracranial pressure may appear early due to limited space (8).

As an extracerebral tumor, LPRM has the imaging characteristics of general meningioma: it often appears as a well-defined circular-like mass; non-contrast CT scanning is mostly more uniform or slightly dense, and calcification is rare; and MR T1WI is an equal or a slightly lower signal, while T2WI is a slightly higher signal, the signal intensity is more uniform, the enhanced scan is more obviously uniformly strengthened, and there may be meningeal tail sign, but this is uncommon (9,10). It has been shown that edema of brain tissue around the tumor is one of the imaging features of LPRM, which is related to the infiltration of a large number of inflammatory cells around the tumor, but it must be noted that peritumoral brain tissue edema is not a unique imaging manifestation of LPRM (11). There is no dura mater in the ventricle, so intraventricular LPRM does not have imaging features of benign meningioma, such as meningeal tail sign and extracerebral tumor mosaic sign (12).

The CT and MR images of this LPRM case were atypical, manifesting as multinodular intraventricular nodules, rough edges, and non-contrast CT scan showing slightly higher density, accompanied by obvious nodular calcification (*Figure 1A*). On T1WI/T2WI and other MR signals, the tumor appeared to adhere to the adjacent lateral ventricular wall, the thalamus was deformed, and perilesional edema was obvious (*Figure 1B,1C*). These obvious aggressive characteristics are, to a certain extent, very similar to those of ependymoma. These confusing imaging manifestations also lead to misjudgments in our imaging diagnosis. However, through postoperative pathological observations, a large number of inflammatory cells and lymphocytes were found in the tumor and its surroundings, as was a small amount of meningeal epithelial component (*Figure 2A,2B*). The finding of EMA (+) may mean that LPRM has both benign and malignant characteristics, similar to anaplastic meningioma (*Figure 2C,2D*); meanwhile, findings of GFAP (–), PR (–), and Ki-67 (+, <1%) indicate that tumor cell proliferation and necrosis are inactive (*Figure 2E-2H*). Finally, the combined findings of vimentin (+) (*Figure 2I*) and other immunohistochemistry results suggest LPRM (WHO grade I).

Differential imaging diagnoses include choroid plexus papilloma, ependymoma, lymphoma, etc. (7,10). Choroid plexus papilloma, which tends to occur in children under 10 years of age, is irregularly lobulated or cauliflower-shaped and is more pronounced after enhancement. Fine granular mixed signals visible inside the choroid plexus papilloma constitute its more characteristic imaging manifestations (13). Ependymoma tends to occur in the lateral ventricle body, the tumor shape is irregular; the border is not clear; it can invade the surrounding brain parenchyma; cystic changes, necrosis, and calcification signs are common; intratumor hemorrhage may occur; and the enhanced scan is mostly uneven and strengthened (14). Primary lymphoma of the brain is more common in middle-

aged and older adult individuals, and the lesions are mostly located around the ventricles and often distributed near the midline, with a clear outline and mild edema being apparent around the lesion (15).

At present, total surgical resection is the best treatment for LPRM, and the probability of recurrence of complete resection is very low; for those who have failed resection, directed radiotherapy is feasible (10,16,17). For the patient described in this case report, the lesion's effect on the surrounding brain parenchyma was quickly relieved following surgery, the patient's symptoms completely disappeared after surgery, the GCS score was good, and the tumor did not recur at 24-month follow-up.

Conclusions

To the best of our knowledge, this is the first case report of multinodular intraventricular LPRMs. This patient is atypical in imaging characteristics, as there were multiple nodules in the ventricles with calcification, no Dural tail sign, and obvious peritumoral edema. These uncommon imaging signs all seriously interfered with our imaging diagnosis. Through this case report, we hope to increase awareness of LPRMs and enhance the vigilance for the rare condition of multinodular LPRMs in the ventricles. The primary physician should improve the timeframe of MRI request and expedite subsequent referral to the local neurosurgical center.

Acknowledgments

The authors sincerely thank the insightful contributions of Yi Liu and Jie Wu who are not listed as co-authors.

Funding: This research was supported by the Foundation of General Hospital of Western Command (No. 2021-XZYG-C04 to Z Zuo and No. 2021-XZYG-C05 to J Zhang).

Footnote

Conflicts of Interest: All authors have completed the ICMJE uniform disclosure form (available at https://qims.amegroups.com/article/view/10.21037/qims-22-1299/coif). ZZ reports that this study was supported by the Foundation of General Hospital of Western Command (No. 2021-XZYG-C04). JZ reports that this study was supported by the Foundation of General Hospital of Western Command (No. 2021-XZYG-C05). The other authors have no conflicts of interest to declare.

Ethical Statement: The authors are accountable for all aspects of the work in ensuring that questions related to the accuracy or integrity of any part of the work are appropriately investigated and resolved. All procedures performed in this case report were in accordance with the ethical standards of the institutional and/or national research committee(s) and with the Helsinki Declaration (as revised in 2013). Written informed consent was obtained from the patient for publication of this case report and accompanying images. A copy of the written consent is available for review by the editorial office of this journal.

References

1. Louis DN, Perry A, Wesseling P, Brat DJ, Cree IA, Figarella-Branger D, Hawkins C, Ng HK, Pfister SM, Reifenberger G, Soffietti R, von Deimling A, Ellison DW. The 2021 WHO Classification of Tumors of the Central Nervous System: a summary. Neuro Oncol 2021;23:1231-51.
2. Tao X, Wang K, Dong J, Hou Z, Wu Z, Zhang J, Liu B. Clinical, Radiologic, and Pathologic Features of 56 Cases of Intracranial Lymphoplasmacyte-Rich Meningioma. World Neurosurg 2017;106:152-64.
3. Louis DN, Ohgaki H, Wiestler OD, Cavenee WK, Burger PC, Jouvet A, Scheithauer BW, Kleihues P. The 2007 WHO classification of tumours of the central nervous system. Acta Neuropathol 2007;114:97-109.
4. Vlodavsky E, Konstantinesku M, Pery-Eran A, Zaaroor M. Meningioma with extensive necrotizing granulomatous changes: possible mimic of inflammatory dural lesions. Histopathology 2004;44:406-8.
5. Kanno H, Nishihara H, Hara K, Ozaki Y, Itoh T, Kimura T, Tanino M, Tanaka S. A case of lymphoplasmacyte-rich meningioma of the jugular foramen. Brain Tumor Pathol 2011;28:341-5.

6. Zhu HD, Xie Q, Gong Y, Mao Y, Zhong P, Hang FP, Chen H, Zheng MZ, Tang HL, Wang DJ, Chen XC, Zhou LF. Lymphoplasmacyte-rich meningioma: our experience with 19 cases and a systematic literature review. Int J Clin Exp Med 2013;6:504-15.
7. Yongjun L, Xin L, Qiu S, Jun-Lin Z. Imaging findings and clinical features of intracal lymphoplasmacyte-rich meningioma. J Craniofac Surg 2015;26:e132-7.
8. Bhatoe HS, Singh P, Dutta V. Intraventricular meningiomas: a clinicopathological study and review. Neurosurg Focus 2006;20:E9.
9. Liu JL, Zhou JL, Ma YH, Dong C. An analysis of the magnetic resonance imaging and pathology of intracal lymphoplasmacyte-rich meningioma. Eur J Radiol 2012;81:968-73.
10. Loh JK, Hwang SL, Tsai KB, Kwan AL, Howng SL. Sphenoid ridge lymphoplasmacyte-rich meningioma. J Formos Med Assoc 2006;105:594-8.
11. Bitzer M, Wöckel L, Morgalla M, Keller C, Friese S, Heiss E, Meyermann R, Grote E, Voigt K. Peritumoural brain oedema in intracranial meningiomas: influence of tumour size, location and histology. Acta Neurochir (Wien) 1997;139:1136-42.
12. Wang YB, Wang WJ, Xu SB, Xu BF, Yu Y, Ma H, Zhang XF. Intraventricular lymphoplasmacyte-rich meningioma: a case report. Turk Neurosurg 2014;24:958-62.
13. Lin H, Leng X, Qin CH, Du YX, Wang WS, Qiu SJ. Choroid plexus tumours on MRI: similarities and distinctions in different grades. Cancer Imaging 2019;19:17.
14. Safai A, Shinde S, Jadhav M, Chougule T, Indoria A, Kumar M, Santosh V, Jabeen S, Beniwal M, Konar S, Saini J, Ingalhalikar M. Developing a Radiomics Signature for Supratentorial Extra-Ventricular Ependymoma Using Multimodal MR Imaging. Front Neurol 2021;12:648092.
15. Kwok HM, Li KY, Chan RLS, Chan CH, Wong SKH, Lee CM, Cheng LF, Ma JKF. Different facets of intracranial central nervous system lymphoma and its imaging mimics. J Clin Imaging Sci 2022;12:4.
16. Bruno MC, Ginguené C, Santangelo M, Panagiotopoulos K, Piscopo GA, Tortora F, Elefante A, De Caro ML, Cerillo A. Lymphoplasmacyte rich meningioma. A case report and review of the literature. J Neurosurg Sci 2004;48:117-24; discussion 124.
17. Firdaus M, Gill AS, Andriani R, Cahyanti D, Yunti MR, Faried A. A rare cystic lymphoplasmacyte-rich meningioma: A case report and review of the literature. Surg Neurol Int 2020;11:391.

Cite this article as: Li G, Wu F, Huang J, Du F, Zhang J, Zuo Z, Jiang R, Yun H, Wang P. Multinodular intraventricular lymphoplasmacyte-rich meningioma with significant calcification: a case description. Quant Imaging Med Surg 2023;13(9):6323-6328. doi: 10.21037/qims-22-1299

